

Three-dimensional bridge-vehicle interaction analysis of simply supported twin I-girder bridge

Trong Le NGO-TRAN*, Toshiro HAYASHIKAWA** and Takashi MATSUMOTO***

* Graduate Student, Graduate School of Eng., Hokkaido University, Nishi 8 Kita 13 Kita-ku, Sapporo 060-8628.

** Dr. of Eng., Professor, Graduate School of Eng., Hokkaido University, Nishi 8 Kita 13 Kita-ku, Sapporo 060-8628.

*** Ph. D., Associate Professor, Graduate School of Eng., Hokkaido University, Nishi 8 Kita 13 Kita-ku, Sapporo 060-8628.

Elaborate three-dimensional finite element models are generated to deal with the bridge-vehicle interaction dynamics of simply supported twin I-girder bridges. The bridge is modeled in detail with solid and shell elements. The studied vehicle is idealized as 3D non-linear model consisting of several lumped masses connected by rigid beams and supported by spring-dampers. Gap and actuator elements are incorporated into the tire models to simulate the separation between the tires and road surface, and road surface roughness, respectively. Correlated road surface roughness profiles are generated from power spectral density (PSD) and cross spectral functions. The models are capable to consider both bridge and vehicle responses with virtually no limitation on the complexity of vehicle and bridge. The dynamic responses of the twin I-girder bridge are extensively investigated under conditions of various roughness classes, vehicle speeds, etc. From numerous calculated results, some useful information regarding to the impact factor of the studied bridge is presented..

Key Words: *Bridge-vehicle interaction; Dynamic load allowance; Twin I-girder bridge;*

1. Introduction

Dynamic behaviors due to vehicles moving across rough surface deck have been long recognized one of the primary concerns in designing and rating of bridges. In spite of its important role, bridge-vehicle interaction dynamic analysis is hardly taken into consideration in practice designs because of its considerable complexity. To account for the dynamic effect, thus, the static response is increased by a single dynamic allowance factor, also known as impact factor that is a function of span length or natural frequency of the bridge only. However, the dynamic response depends on many parameters such as dynamic properties of bridge and vehicle, roughness of bridge surface, speed of moving vehicle, etc. Therefore, this approach is certainly an oversimplification and, in many cases, misrepresentation of the sophisticated phenomena involved in the bridge-vehicle interactions¹⁾.

By this reason, bridge-vehicle interaction has been intensively studied by many researchers using both experimental tests and sophisticated numerical models to refine the impact factor during the last three decades. A series of papers dealing with the numerical methods for bridge-vehicle interaction were presented by Yang et al.^{2,3,4,5)}. In this series, the interaction dynamics are treated by

simple numerical methods for reducing computational cost as well as versatile method that can handle the bridge-vehicle system with practically no limit on the level of complexity. Another series of papers studying about the dynamic response of multi-girder bridges were published by both Huang et al.^{6,7)} and Wang et al.⁸⁾. These papers investigated the impact factor of multi-girder bridges with different span lengths. Bridges were idealized as grillage beam systems and the vehicle was as a nonlinear vehicle model with 12 degrees of freedom according to the HS20-44 truck design loading of American Association of State Highway and Transportation Officials specifications (AASHTO). Many useful results for bridge design and further study were achieved from these researches. Recently, Kim et al.⁹⁾ presented a 3-D means of analysis for bridge-vehicle interaction. The results calculated by using beam and plate elements with the proposed method were well correlated with experimental results. The cited studies and many others have made valuable contributions to better understandings of the bridge-vehicle interaction problem. However, almost all of the analyses used in these studies relied on specialized, local developed computer programs that were intended primarily for research use. Therefore, these programs have limited utility for most practical bridge engineers. A study that utilized completely a

commercially available computer LS-DYNA code was presented by Kwasniewski et al.¹⁰⁾. However, no road roughness was taken into account in this paper. Other attempts that used the commercial ANSYS code throughout were reported by Barefoot et al.¹¹⁾ and Martin et al.¹²⁾. However, these reports used relative simple moving loads instead of moving spring-mass-dampers and no roughness was mentioned.

Although there have been a lot of researches on this problem, there is still no single formula to predict the impact factor for any types of bridge. For these reasons, this paper presents elaborate three-dimensional finite element models used within commercially available ANSYS code to parametrically study the bridge-vehicle interaction of composite twin I-girder bridges, which have been considered as one of the efficient types and one of the most popular bridge types for short and medium span highway bridges in Japan¹³⁾. The models are capable to consider both bridge and vehicle responses with virtually no limitation on the complexity of vehicle and bridge. Effects of various parameters on the dynamic load allowance of the studied bridge are presented.

2. Analytical Models

In this study, the commercial ANSYS 10.0 code was chosen. This code provides a vast capability for both static and dynamic analyses, a numerous element types, and especially an advanced contact technology. This code, moreover, is integrated with a scripting language, ANSYS Parametric Design Language (APDL), which can be used to automate common tasks or even build models in terms of parameters (variables).

2.1 Twin I-girder bridge

Composite steel twin I-girder bridges have been considered as one of the efficient and popular types of highway bridge because of its simplicities in design and fabrication, speed of construction as well as low cost for maintenance¹³⁾. However, this type of bridge structure has low torsional rigidity; it is susceptible to vibrate by external dynamic loads. The bridge chosen in this study is a simply

supported, composite, steel twin I-girder, 2-lane one whose span is 50m. The two main I-girders are 3m deep and spaced transversely at 6m. These main structural members are tied together by a pre-stressed concrete slab of 30cm thick, which is assumed to act compositely with the girders, and eleven transverse cross-beams which are spaced equally along the span. Although the simply supported bridge is not representative of all types of bridges, it embodies many of the important dynamic characteristics of bridges. Basic geometric properties and cross-section layout and of the studied bridge are presented in Table 1 and Fig. 1, respectively.

Bridge structures can be idealized in many different ways. Herein, detailed finite element model is selected to analyze the interaction problems. Hexagonal 8-node elements are used for concrete deck and quadrilateral 4-node shell elements with 6 dofs at each node are for all steel members. Lumped mass system and Rayleigh damping¹⁴⁾ are assumed in these analyses. Based on the experimental results of the approximately same bridges^{6,8,13)}, one percent of critical damping is assumed for the first and second modes in most of the analyses.

2.2 AASHTO HS20-44 vehicle

Vehicular live loading on bridges specified in AASHTO LRFD2004, designated HL93, consists of a combination of the design truck HS20-44 or design tandem and design lane load¹⁵⁾. Only the static effects of the design truck and tandem are increased by a factor, called dynamic load allowance, to take into account the dynamic effects. Figure 2 shows the weights and spacings of axles for the HS20-44 design truck and its finite element model. The spacing between the two 145kN axles can be varied between 4.3m and 9.0m to produce unfavorable effects.

The design truck is idealized as a 3-D nonlinear finite element model consisting of masses connected by rigid beams and supported by spring-dampers. Five lumped masses, which are 3-D masses with rotary inertias, represent for the tractor, semi-trailer, and three wheel/axle sets. The upper spring-dampers represent the suspensions of the vehicle and the lower ones are for tires. Properties of the masses and spring-dampers can be found in a report of Wang

Table 1 Basic geometric properties of the studied bridge

Span length [m]	50
Deck width x thickness [m]	10.5 x 0.3
Dimensions of the main girders [mm]	WEB 3000x24 Upper FLG 500x30 Lower FLG 500x50
Dimensions of the intermediate cross-beams [mm]	WEB 1000x16 FLG 300x25
Dimensions of the end diaphragms [mm]	WEB 3000x16 FLG 300x25

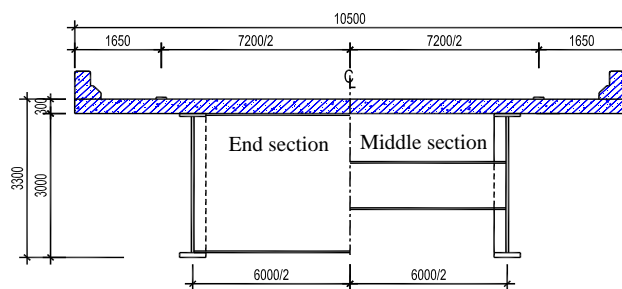


Fig. 1 Cross sections of the studied bridge (mm)

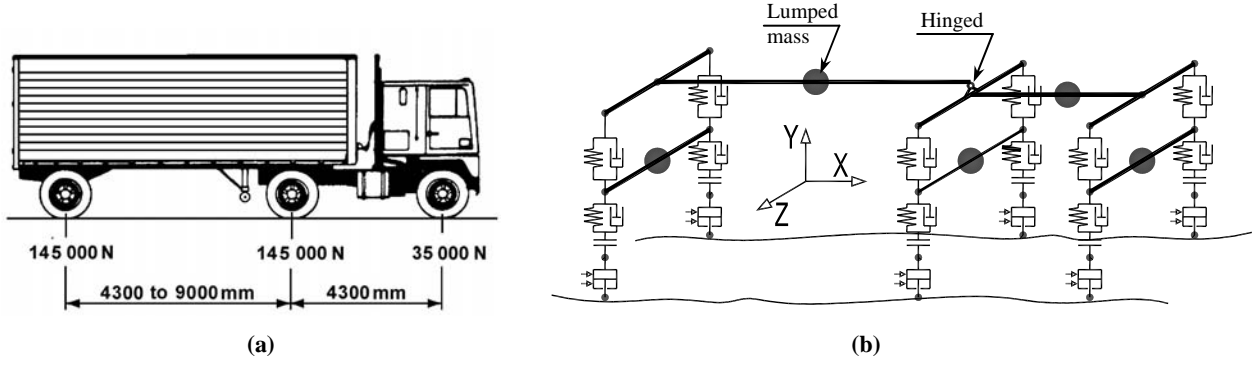


Fig. 2 HS20-44 design truck: (a) General configuration and (b) Finite element model

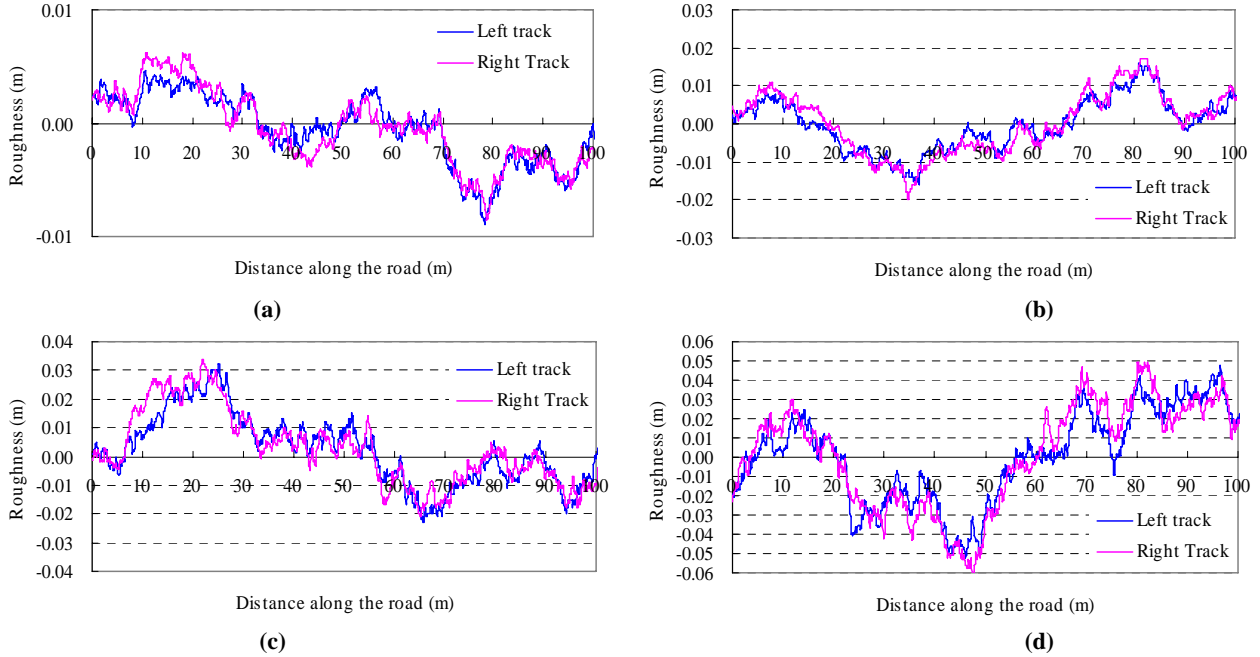


Fig. 3 Road roughness profiles: (a) very good; (b) good; (c) average; and (d) poor road classes

and Huang¹⁶). Gap elements are incorporated to the lower spring-damper elements to imitate the separation between tires and road surface. These gap elements, in turn, are interconnected with actuators elements to simulate the effects of road surface roughness. It can be seen that the vehicle model are capable to take into account the effects of pitching, rolling, bouncing of vehicle body as well as the effect of separations between tires and road surface.

2.3 Road surface roughness

There is no doubt that road surface roughness plays an important role in the dynamic responses of bridge-vehicle system. In this study, road surface profiles are assumed to be periodically modulated random processes that can be described by a power spectral density function (PSD). The PSD function of road surface roughness on bridges can be approximated by an exponential function^{17,18}) as

$$S(n) = S(n_0) \left(\frac{n}{n_0} \right)^{-w} \quad (1)$$

where: $S(n)$ = PSD ($\text{m}^2/\text{cycle}/\text{m}$); n = wave number (cycle/m); $S(n_0)$ = roughness coefficient ($\text{m}^2/\text{cycle}/\text{m}$). In this

study, $S(n_0) = 5\text{E-}6, 20\text{E-}6, 80\text{E-}6$ and $320\text{E-}6$ for very good, good, average and poor road surfaces, respectively, according to the values recommended by MIRA¹⁷); n_0 = discontinuity frequency = $1/(2\pi)$ (cycle/m). The value of w is varied from 1.36 to 2.28¹⁷) depended on the road class. For the principal roads, w is 2.05 when $n \leq n_0$ and 1.44 when $n > n_0$. For simplicity, w can be assumed the value of 2^{8,16}).

A popular method for generating a random profile that is approximately stationary from a PSD function is by summing a large number of sinusoids¹⁹) as

$$y(x) = \sum_{i=1}^N \left[\sqrt{\Delta n_i \cdot S(n_i)} \cdot \cos(2\pi \cdot n_i \cdot x + \phi_i) \right] \quad (2)$$

where: x = longitudinal distance; N = the number of sinusoidal components used to generate the profile; n_i = the spatial frequency associated with the i^{th} component; Δn_i = the bandwidth of the i^{th} component; and ϕ_i = a random phase angle uniformly distributed from 0 to 2π . Typically, the components should cover the wave number range from 0.011cycle/m to 3.281cycle/m¹⁹).

Most vehicles travel over two wheel tracks, and thus subjected to two simultaneous road surface profiles to include bouncing, pitching (rotation about transverse axis), and rolling (rotation about longitudinal axis) effects of its body. In this study, correlated road surface profiles are generated from PSD and cross spectral density functions by assuming road surface as homogeneous and isotropic random process^{17,19,20}. The approach is to build the profile from several uncorrelated components, and use the cross-spectral density function to determine the relative contribution of each as described in Eq. (3) as

$$y_R(x) = \sum_{i=1}^N \left[\frac{\sqrt{\Delta n_i \cdot S_x(n_i)} \cdot \cos(2\pi n_i x + \phi_i) + \sqrt{\Delta n_i \cdot (S(n_i) - S_x(n_i))} \cdot \cos(2\pi n_i x + \theta_i)}{\sqrt{\Delta n_i \cdot S_x(n_i)} \cdot \cos(2\pi n_i x + \phi_i) + \sqrt{\Delta n_i \cdot (S(n_i) - S_x(n_i))} \cdot \cos(2\pi n_i x + \theta_i)} \right] \quad (3)$$

where: $S_x(n)$ = cross spectral density; ϕ_i = a random phase angle uniformly distributed from 0 to 2π used for the first profile; and θ_i = a second random phase angle uniformly distributed from 0 to 2π .

It could be seen that the correlated components of the second profile are produced by the first term and the uncorrelated ones are by the second term. From these equations, several road roughness profiles are generated for every very good, good, average, and poor roads typically shown on Fig. 3.

3. Analytical Results

3.1 Free vibration analysis

The usual first step in performing a dynamic analysis is determining the natural frequencies and mode shapes of the structure with damping neglected. Although this process does

not relate to any loadings, its results characterize the basic dynamic behavior of the structure and are an indication of how the structure will respond to dynamic loadings. Figures 4 and 5 show several important mode shapes along with their frequencies of the studied vehicle and bridge, respectively. It can be seen that the frequencies of the vehicle are close to those of the bridge; this could cause the interaction between these systems more unfavorable.

3.2 Parametric study

To model the vehicle running on the bridge deck, ANSYS surface-to-surface contact elements are employed. This advanced contact technique allows contact surfaces to slide on the target surfaces with or without friction. Correlated road roughness generated by Eqs. 2 and 3 is input as stroke (length) of the actuator elements to simulate the unevenness of road surface. In each class of road surface, several correlated roughness profiles are analysed to get the mean values of the dynamic responses. To get the initial displacements, velocities and accelerations of the vehicle when entering the bridge, the vehicle is run on an approach road of 45m long with the same road surface roughness. Figure 6 shows static and dynamic deflection histories of the two girder mid-spans under asymmetric lane position, vehicle moving at 60km/h on good road surface. The dynamic load effect in this study is measured in terms of maximum deflections. The dynamic load allowance (IM) is defined as

$$IM(\%) = \left(\frac{R_{Dyn.} - R_{Sta.}}{R_{Sta.}} \right) \times 100\% \quad (4)$$

in which $R_{Dyn.}$ and $R_{Sta.}$ are the absolute maximum responses of dynamic and static, respectively as shown in Fig. 6.

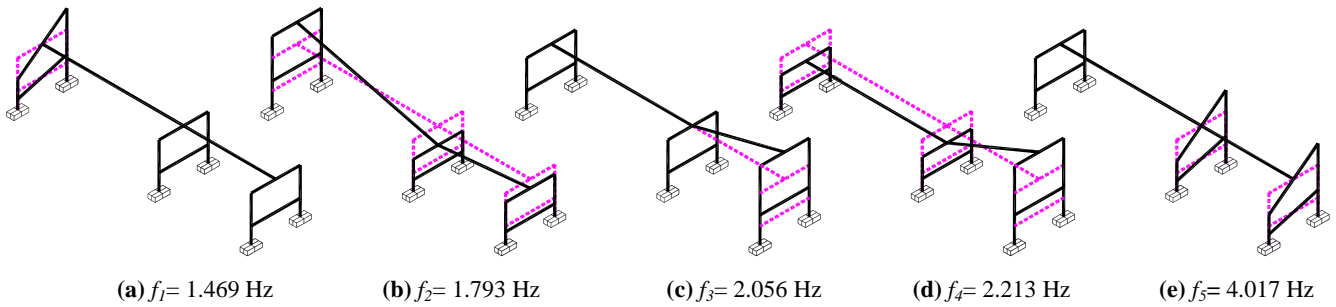


Fig. 4 Several mode shapes of the studied vehicle

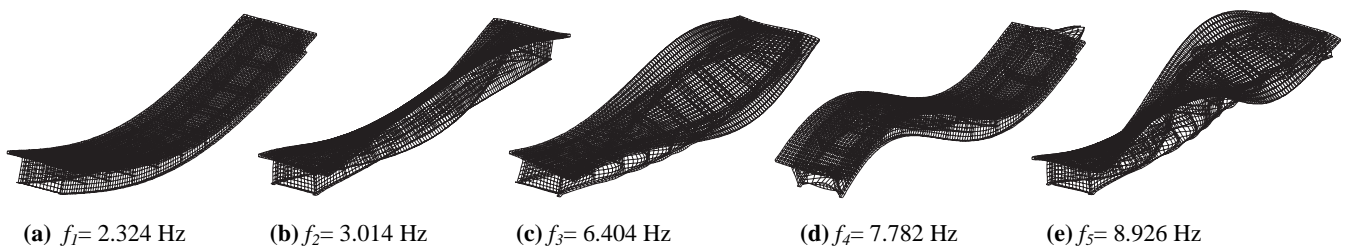


Fig. 5 Several mode shapes of the studied bridge

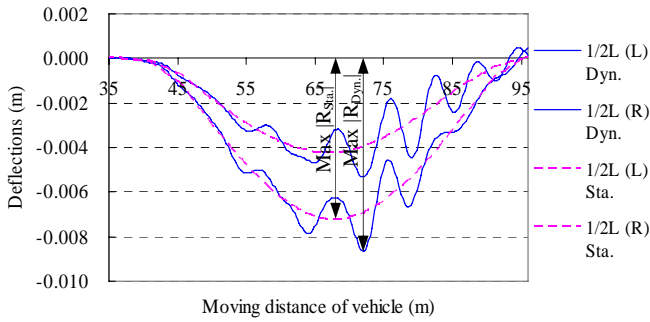


Fig. 6 Deflection history at mid-span ($v = 60\text{km/h}$, good road surface)

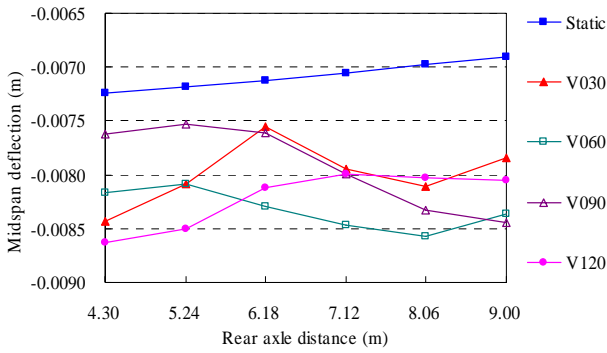


Fig. 8 Static and dynamics deflections versus rear axle distance (good road surface)

(1) Effect of loading position

The studied bridge was designed for two identical traffic lanes separated by the centre line of bridge deck as depicted in Fig. 1. However, to study the effect of loading position, two loading cases are considered: the designed asymmetric loading case which runs over the right girder and another symmetric loading case whose centre moves along the centre line of the bridge deck. Four classes of road roughness in each lane and four vehicle speeds in each road class are carried out.

Figure 7 shows a typical dynamic allowance of the left (L) and right (R) girders subjected to the two studied loading lanes (Sym. and Asym. lanes) with different vehicle speeds running on good road surface condition. It can be seen in the figure that the highest and lowest dynamic allowances are always those of the left and right girders in asymmetric loading case, respectively; those from symmetric loading case are in the middle regardless of vehicle speed and road roughness class. It is necessary to remind that the asymmetric lane runs on the right side of bridge deck. Therefore, it can be said that the larger the static response is, the smaller the dynamic allowance can be obtained. This was also mentioned in many previous papers^{7,8}. Although having higher dynamic load allowances, the maximum tensile stresses at the mid-span of the left girder in asymmetric and both girders in symmetric cases are always smaller than that of the right girder in asymmetric loading case. They are about 60% and 80% of the right girder's stress in asymmetric case, respectively. Because only one value of dynamic allowance is usually used for all girders and both girders are designed identically, it is reasonable to use dynamic load allowance of

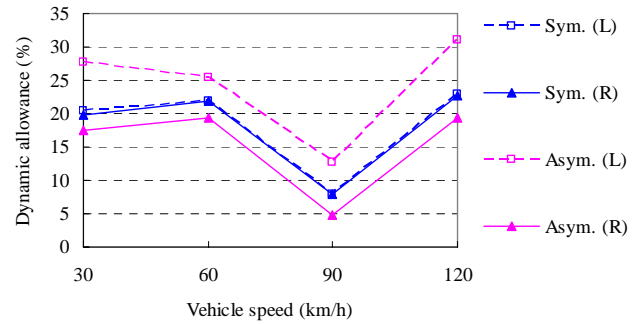


Fig. 7 Dynamic allowance of studied loading cases with different speeds (good road surface)

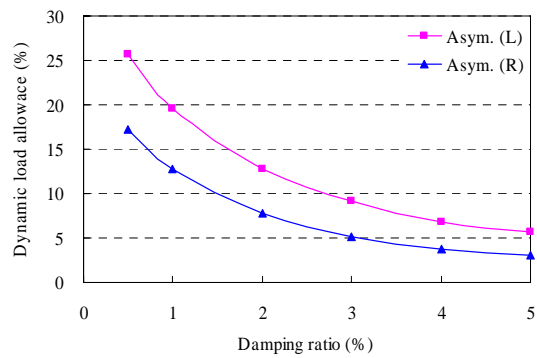


Fig. 9 Dynamic load allowance versus damping ratio ($v = 60\text{km/h}$, good road surface)

right girder in asymmetric loading case for the unique dynamic load allowance of the studied bridge.

(2) Effect of vehicle length

As mentioned in Fig. 2a, the spacing between the two 145kN axles can be varied between 4.30 m and 9.00 m to produce unfavorable effects. In static analysis of simply supported bridges, it is easy to know that the shorter the spacing is, the larger the response can be achieved. However, in these analyses, it is not that ease because the dynamic interaction between bridge and vehicle depends on many factors such as dynamic properties of bridge/vehicle, bridge roughness, vehicle speed etc. In this section, six different axle spacings between the two rear ones ranging from 4.30m to 9.00m are analyzed in every four vehicle speeds. Except the different in rear axle spacing, all other properties of bridge and vehicle remain unchanged. The road is assumed as good surface class.

Maximum static and dynamic deflections of mid-span with various axle distances are plotted on Fig. 8. It can be seen that the static response decreases with the increase of rear axle spacing as expected; whereas, the dynamic ones are scattered and almost unpredictable. The dynamic load allowances seem to achieve the maximum values in shorter axle distance when vehicle speeds are 30 and 120 km/h and vice versa when vehicle running at 60 and 90 km/h. They are in the range of 6-16%, 13-23%, 5-22% and 13-19% corresponding to the vehicle speeds of 30, 60, 90 and 120km/h, respectively.

(3) Effect of damping

Damping plays an important role in reducing vibrations in any dynamic problems. However, this value is usually measured directly on the real structure and cannot be specified at the analysis stage. Therefore, it is common to adopt a damping ratio that is measured from similar structures for current dynamic analyses. In all previous analyses, one percent of critical damping is assumed for the first and second modes. In this section, six values of damping ratio ranging from 0.5% to high value of 5% are carried out to study the effect of damping although the damping ratio of the studied bridge structure is not that high.

The calculated results under the conditions of good road surface and 60km/h are graphically presented in Fig. 9. From the figure, the dynamic load allowance decreases with the increase of damping ratio. The effect of damping is significant; however, its influence is not linear. The larger the damping ratio is, the smaller the changing rate of dynamic allowance will be. In addition, the difference of dynamic allowance between the left and right girders becomes smaller when increasing the damping ratio.

(4) Effect of correlated roughness profile

There is no doubt that road surface roughness plays an important role and cannot be neglected in the dynamic response of bridge-vehicle systems. Most vehicles travel over two wheel-tracks, and are thus subjected to two simultaneous different roughness profiles. It is widely accepted that the two profiles are correlated (correlated model) with each other¹⁷. However, a larger number of bridge-vehicle analyses used the same roughness profile for both wheel-tracks (perfectly

correlated model), ignored the vehicle width and roll motion (longitudinal twisting) of the vehicle body; others employed two completely different profiles (uncorrelated model). Both of the latter models do not reflect the real world. But, for simplicity, they are still used widely in the field of bridge-vehicle interaction.

In this section, the perfectly correlated and correlated road roughness models are investigated. The perfectly correlated profiles are extracted from the left ones of the correlated models. Figure 10 shows the differences of dynamic load allowances between correlated and perfectly correlated roughness models with various vehicle speeds and road surface classes. It can be observed that the difference between these roughness models is small and negligible under very good, good and average road surface conditions. However, under poor road conditions, the effect of correlated roughness model becomes significant. The difference can be as high as +26% when vehicle running at 30km/h on poor road surface. This large difference can be explained for the contribution of the roll mode of vehicle on poor road surface in combination with low torsional stiffness of the studied twin I-girder bridge. Under other road conditions, because of the small difference between the two correlated profiles, the participation of the vehicle roll mode on dynamic allowance is small. In addition, the correlated roughness model slightly reduces the dynamic effect of vehicle pitch mode. By these reasons, the response of mid-span with correlated roughness model is smaller than that with perfectly correlated roughness as clearly shown in Fig. 10 in the cases of very good and good surfaces.

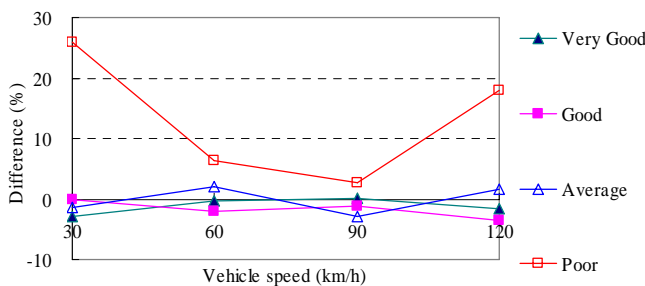


Fig. 10 Difference of dynamic load allowance between correlated and perfectly correlated roughness profiles

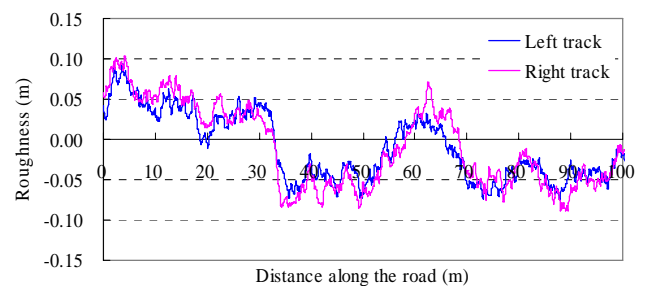


Fig. 11 Very poor road roughness profiles

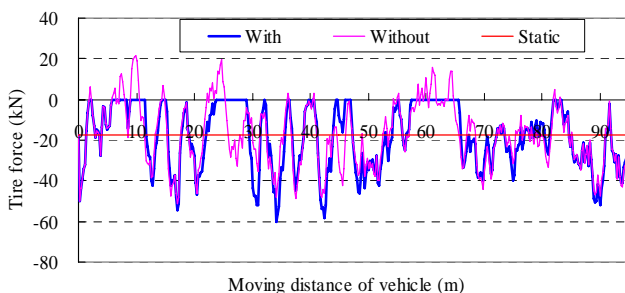


Fig. 12 Tire force histories of the right front wheel with and without tire bouncing effects

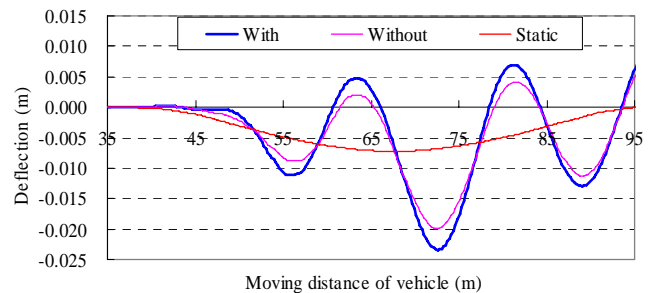


Fig. 13 Mid-span deflection histories of the right girder with and without tire bouncing effects

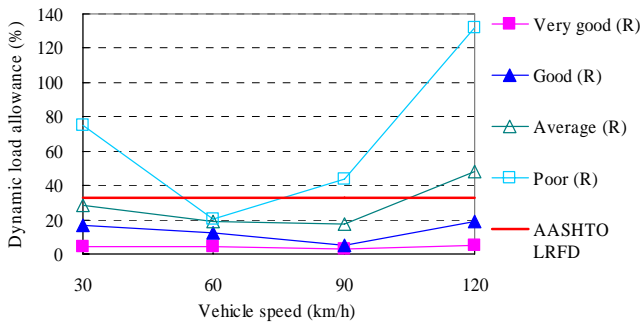


Fig. 14 Dynamic load allowance with different road surface classes and vehicle speeds

(5) Effect of tire bounce

In all of the previous analyses, the tire forces of entire wheels still remain in compression even when running at 120km/h on the poor road surface. That means all the tires are still in contact, no separation with the road surface. In these cases, it is unnecessary to simulate the bounce of tires. However, this is very important in analysing the interaction between a vehicle and an old bridge with bumps at expansion joints or potholes on its surface for load ratings or life calculations.

To verify the possibility of this vehicle model in simulating the tire bouncing effects, another very poor surface whose roughness coefficient is $1280E-6$ ($m^2/cycle/m$) is considered and plotted on Fig. 11. A new vehicle model without the gap elements that are for simulating the bouncing effects is studied together with the aforementioned model. In both cases, the vehicles run at the high speed of 120km/h. The tire force histories of the front right wheels in with and without gap elements are shown on Fig. 12. As shown on the figure, the gap elements successfully model the effects of tire bounce off the road surface. No tensile force can exist in vehicle model with gap elements. The calculated result histories of mid-span deflection under the two vehicle models are presented in Fig. 13. As can be seen, the maximum response of mid-span in the case of vehicle model with gap elements is approximately 18% larger than that of the model without these elements. This could be explained for the hammering effects when vehicle tires get into contact with the road surface after bouncing.

(6) Effects of vehicle speed, road surface and maximum dynamic load allowance of the studied bridge

This section extensively studies the dynamic load allowance of the studied bridge under various vehicle speeds and road surfaces conditions. Four classes of road roughness along with four different vehicle speeds are analyzed. In each roughness class, several profiles are considered to get the mean values of dynamic load allowances. Asymmetric loading lane and shortest vehicle configuration are used.

Figure 14 illustrates the variation of the dynamic load allowance of the two main girders with varying road surface classes and vehicle speeds. Regardless the road surface classes, the dynamic load allowances fluctuate with the increase of vehicle speeds. However, they seem to achieve their maximum values at the fastest studied speed of 120km/h, and the second highest values are at the lowest studied speed of 30km/h. Except the dynamic load allowances under poor road condition, that take the minimum values at 60km/h, the remaining ones appear to fall to lowest values at 90km/h.

The figures also exhibit that the dynamic load allowance is greatly influenced by road surface conditions. It is unquestionable that the worse the road surface is, the higher the dynamic load allowance will occur. In this study, the dynamic load allowances can reach very high value of approximately 130% when vehicle running at the fastest studied speed on the worst studied surface conditions. These calculated results are also compared with the one specified in AASHTO LRFD 2004 specifications¹⁵. With very good and good road surfaces, the dynamic load allowances of all girders are well below the value given by specifications. In the cases of average and poor surfaces, the AASHTO LRFD seems to underestimates the dynamic load allowance of the studied bridge.

4. Conclusions

The bridge-vehicle interaction dynamic of simply supported twin I-girder bridge is extensively studied by using ANSYS code which is commercially available and well known among practical engineers. The developed models are capable to take into account many important factors involving bridge-vehicle interaction problem such as effects of bouncing, rolling, pitching of vehicle body, separating between tires and road surface; as well as road surface roughness conditions. There is virtually no limitation on the degree of complexity of vehicle and bridge. The calculated results provide sufficient evident for the following conclusions:

From the analyses of different lane loadings, it could be seen that the larger the static response is, the smaller the dynamic allowance can be obtained. Because only unique value of dynamic allowance is usually used for all girders, it is reasonable to use dynamic load allowance of the right girder in asymmetric loading case.

Vehicle lengths greatly influence the dynamic responses of the studied bridge. While the static response decreases with the increase of rear axle spacing as expected, the dynamic ones are scattered and almost unpredictable.

Dynamic load allowance decreases with the increase of damping ratio. The larger the damping ratio is, the smaller the changing rate of dynamic allowance will be. In addition, the difference of dynamic allowance between the left and right girders becomes smaller when increasing the damping ratio.

The bridge-vehicle model successfully simulates the effect of separations between tires and road surface. The response of mid-span in the case of vehicle model with separation effects is more significant because of hammering effects when vehicle tires get to contact with the road surface after bouncing. However, there is no separation between these surfaces in conventional analyses with good, very good, average and poor road classes at studied speeds.

It can be observed that regardless of the road surface classes, the dynamic load allowance fluctuates with the increase of vehicle speed. However, it seems to archive the maximum ones at the fastest and lowest studied speeds. The results also exhibit that the dynamic load allowance is greatly influenced by road surface conditions. The worse the road surface is, the higher the dynamic load allowance will be. With very good and good road surfaces, the dynamic load allowances of all girders are well below the value given by specifications. In the cases of average and poor surfaces, the AASHTO LRFD seems to underestimate the dynamic load allowance of the studied bridge.

References

- [1] Yang, Y. B., Liao, S. S. and Lin B. H., Impact formulas for vehicles moving over simple and continuous beams, *Journal of Structural Engineering*. Vol. 121 (11), pp.1644-1650, 1995.
- [2] Yang, Y. B. and Lin, B. H., Vehicle-bridge interaction analysis by dynamic condensation method, *Journal of Structural Engineering*. Vol. 121(11), pp.1636-1643, 1995.
- [3] Yang, Y. B. and Yau, J. D., Vehicle-bridge interaction element of dynamic analysis, *Journal of Structural Engineering*. Vol. 123(11), pp.1512-1518, 1997.
- [4] Yang, Y. B., Chang, C. H., and Yau, J. D., An element for analysing vehicle-bridge systems considering vehicle's pitching effect, *International Journal for Numerical Methods in Engineering*. Vol. 46, pp.1031-1047, 1999.
- [5] Yang, Y. B. and Wu, Y. S., A versatile element for analysing vehicle-bridge interaction response, *Engineering Structures*. Vol. 23, pp.452-469, 2001.
- [6] Huang, D., Wang, T. L., and Shahawy, M., Impact analysis of continuous multigirder bridges due to moving vehicles, *Journal of Structural Engineering*. Vol. 118 (12), pp. 3427-3443, 1992.
- [7] Huang, D., Wang, T. L., and Shahawy, M., Impact studies of multigirder concrete bridges, *Journal of Structural Engineering*. Vol. 119 (8), pp.2387-2402, 1993.
- [8] Wang, T. L., Huang, D., and Shahawy, M., Dynamic response of multigirder bridges, *Journal of Structural Engineering*. Vol. 118 (8), pp.2222-2238, 1992.
- [9] Kim, C. W., Kawatani, M., and Kim, K. B., Three-dimensional dynamic analysis for bridge-vehicle interaction with roadway roughness, *Computers and Structures*. Vol. 83, pp.1627-1645, 2005.
- [10] Kwasniewski, L., Li, H., Wekezer, J., and Malachowski, J., Finite element analysis of vehicle-bridge interaction. *Finite Elements in Analysis and Design*. Vol. 42, pp.950-959, 2006.
- [11] Barefoot, J. B., Barton, F. W., Baber, T. T., and McKeel, W. T., Development of finite element models to predict dynamic bridge response, *Final report - Virginia Transport Research Council*. Charlottesville Virginia, USA, 1997.
- [12] Martin, T. M., Barton, F. W., McKeel, W. T., Gomez, J. P. , and Massarelli, P. J., Effect of design parameters on the dynamic response of bridges. *Final report - Virginia Transport Research Council*. Charlottesville Virginia, USA, 2000.
- [13] Kim, C. W., Kawatani, M., and Hwang, W. S., Reduction of traffic-induced vibration of two-girder steel bridge seated on elastomeric bearings, *Engineering Structures*. Vol. 26, pp.2185-2195, 2004.
- [14] Clough, R. W. and Penzien, J., *Dynamics of Structures*, Computers and Structures, Inc., 2003.
- [15] The American Associate of State Highway and Transportation Officials, *AASHTO LRFD Bridge Design Specifications*. 2004.
- [16] Wang, T. L. and Huang, D., Computer modeling analysis in bridge evaluation, *Final report - Highway Planning and Research Program*. Miami, Florida, 1992.
- [17] Dodds, C. J. and Robson, J. D., The description of road surface roughness, *Journal of Sound and Vibration*. Vol. 31(2), pp.175-183, 1973.
- [18] Honda, H., Kajikawa, Y., and Kobori, T., Spectra of road surface roughness on bridges, *Journal of the Structural Division (ASCE)*. Vol. 108(ST9), pp.1956-1966, 1982.
- [19] Sayers, M. W., Dynamic terrain inputs to predict structural integrity of ground vehicles, *Technical report - Transportation Research Institute*. The University of Michigan, 1988.
- [20] Kamash, K. M. A. and Robson, J. D., The application of isotropy in road surface modeling, *Journal of Sound and Vibration*. Vol. 57(1), pp.89-100, 1978.

(Received September 18, 2007)